PHYSICAL REVIEW B **71**, 060403(R) (2005)

Strain-induced crossover of the metal-insulator transition in perovskite manganites

Y. Ogimoto,[1,*] M. Nakamura,[2] N. Takubo,[2] H. Tamaru,[3] M. Izumi,[3] and K. Miyano[3]
[1]*Devices Technology Research Laboratories, SHARP Corporation, Nara 632-8567, Japan*
[2]*Department of Applied Physics, The University of Tokyo, Tokyo 113-8656, Japan*
[3]*Research Center for Advanced Science and Technology, The University of Tokyo, Tokyo 153-8904, Japan*
(Received 19 October 2004; published 16 February 2005)

The essential role of strain in determining the electronic states of perovskite manganites is clearly demonstrated in the form of anisotropic and substrate-dependent crossover of a first-order phase transition in charge-orbital ordered epitaxial thin films of $(Nd_{1-x}Pr_x)_{0.5}Sr_{0.5}MnO_3$. An application of (110)-oriented epitaxial growth technique allows the structural flexibility indispensable for the large anisotropic lattice deformation at the first-order transition. The technique enables us to fine-tune the Jahn-Teller distortion for manipulating the metal-insulator transition in thin films, a first step toward the strongly correlated electron devices.

DOI: 10.1103/PhysRevB.71.060403 PACS number(s): 75.70.−i, 75.40.−s, 75.47.−m, 78.66.−w

Physics associated with strain underlies the colossal magnetoresistance and other gigantic changes in magnetic, resistive, and optical properties in perovskite manganites.[1–3] Since the Jahn-Teller (JT) coupling, one salient aspect of strain physics, is an essential interaction in the charge-orbital ordered (COO) manganites;[4,5] pseudomorphic strain effect in epitaxial manganite thin films[6–8] is a unique degree of freedom for the control of subtle situation in a multicritical point.[9,10] One noticeable example is the drastic modification of the ground state of $La_{0.5}Sr_{0.5}MnO_3$ thin films coherently grown on a (001) surface; they are located close to the phase boundary and the modification is driven by the biaxial strain through the orbital ordering (OO).[8] Hence the tetragonal modification in thin films has been recognized as an important parameter to characterize the electronic phase diagram in the theoretical studies.[11] However, there has been no report on the epitaxial thin films that are amenable to the control of the *first-order* metal-insulator (MI) transition arising from the COO. The difficulty arises partly from modification of the ground state by imposing tetragonal symmetry, and partly from severe restriction on the lattice deformation, in which only the out-of-plane lattice constant can vary at the MI transition while the in-plane lattice constants are clamped to the substrates.[12] This makes it quite difficult for the films to undergo the transition into the COO state since a large anisotropic deformation is unavoidable at the transition. Although not frequently addressed to, anisotropy is in fact an essential factor even in a pseudocubic lattice when OO is encountered. In a few forerunning attempts employing carefully prepared "twin-free" single crystal samples,[13,14] a close connection has been revealed between the OO and the anisotropic properties, which are undetectable in the conventional multidomain samples. Incidentally, it is to be noted that in the case of polycrystalline films, in which one might expect that the restrictions for the epitaxial films mentioned above are absent, first-order MI transition does not appear because of the random field effect arising from defects and grain boundaries. In $Nd_{0.5}Sr_{0.5}MnO_3$ films, for example, the charge ordered (CO) state existing within the narrow hole concentration range ($0.49 \leqslant x \leqslant 0.51$) (Ref. 15) collapses quite easily by the polycrystalline disorder[16] and the CO state is wiped out.

Here, we report on the strain-induced crossover of a first-order MI transition in thin films by an application of *(110)-oriented epitaxial growth technique* to $(Nd_{1-x}Pr_x)_{0.5}Sr_{0.5}MnO_3$ (NPSMO),[15] which can be viewed as being in a bicritical state between *CE*-type $[d(3x^2-r^2/3y^2-r^2)]$ ($x=0$; $Nd_{0.5}Sr_{0.5}MnO_3$) (Refs. 17–19) and *A*-type $[d(x^2-y^2)]$ ($x=1$; $Pr_{0.5}Sr_{0.5}MnO_3$) states.[18,20,21] In the present paper, $SrTiO_3$ (STO) and $[(LaAlO_3)_{0.3}-(SrAl_{0.5}Ta_{0.5}O_3)_{0.7}]$ (LSAT) (110) perovskite substrates were employed. The difficulties associated with the tetragonal substrates are averted by breaking the in-plane symmetry: the in-plane anisotropy allows the lattice deformation compatible with the modified OO plane lying out of the substrate surface (see below). The mode of deformation also determines the type of the crossover of the MI transition. One is the in-plane anisotropic crossover for the films on STO utilizing the unequivalent in-plane lattice constants $[d(001) \neq \sqrt{2}d(1\text{-}10)]$ due to the anisotropic lattice relaxation, and the other is the substrate-dependent crossover between the films on STO and LSAT substrates.

We have grown NPSMO films by the pulsed-laser deposition technique with typical conditions for manganite thin films as described in the literature.[8] The bandwidth has been delicately tuned by varying the Pr content ($x=0$, $1/3$, $1/2$, and 1). The thickness of the films was in the range of 50−110 nm in which there are no essential thickness-dependent properties. The surface of the (110) substrates cannot be regulated on an atomic scale with a step and terrace structure, as is known for (001) perovskite substrates,[22] but is smooth enough to observe the intensity oscillation of reflection high-energy electron diffraction (RHEED) all through the growth of the films on LSAT ($a=0.387$ nm, mismatch $=0.7\%$). Coherent epitaxial growth was confirmed by four-circle x-ray diffraction measurements, which indicate that the films on LSAT have the identical in-plane lattice constants to [001] and [1-10] axes of the substrates, respectively. As for the films on STO ($a=0.3905$ nm, mismatch $=1.6\%$) substrates, the lattice mismatch is too large to keep coherent epitaxial growth, resulting in the appearance of streak RHEED pattern that still assures a smooth surface on nanometer scale. The films have nearly the same lattice con-

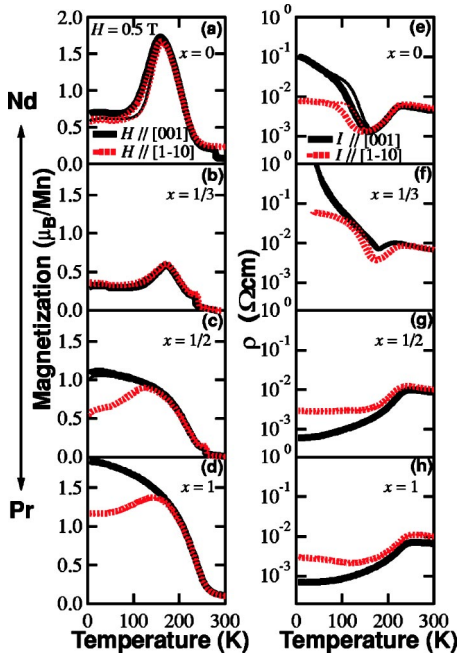

FIG. 1. (Color online) (a)–(d) Left panels show temperature (T) dependence of magnetization (M), for $(Nd_{1-x}Pr_x)_{0.5}Sr_{0.5}MnO_3$ epitaxial thin films on $SrTiO_3$ (110) substrates. M is measured by a superconducting quantum interference device magnetometer with zero-field-cooled (ZFC) field-warming (thin line) and FC (thick line) runs applying a magnetic field (H) of 0.5 T along the [001] and [1-10] directions denoted by solid and dotted lines, respectively. (e)–(h) The right panels exhibit T dependence of resistivity (ρ) measured with ZFC (thick line) and ZFW (thin line) runs by a conventional four-probe method.

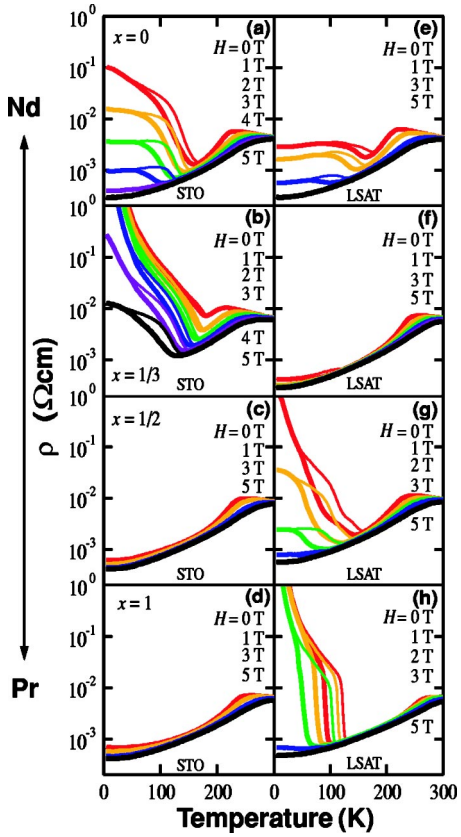

FIG. 2. (Color online) (a)–(d) Left panels show ρ-T curves for NPSMO films on STO substrates, measured with FC (thick line) and FW (thin line) runs applying a various magnetic field of 0–5 T along the [001] direction. (e)–(h) The right panels show ρ-T curves for the films on LSAT.

stant to the substrate along [001] axis but two types of domains with slightly tilted [110] axes toward [001] and [00-1] directions are sometimes observed.[23] The lattice is largely relaxed along [1-10] axis. Thus, we have two types of films; one type is epitaxial films on STO with anisotropic in-plane lattice constants, and another is coherently grown epitaxial films in the form of a monodomain crystal on LSAT with rather isotropic in-plane lattice constants clamped to the substrates.

Figure 1 systematically displays the magnetic [Figs. 1(a)–1(d)] and transport [Figs. 1(e)–1(h)] data for the NPSMO films on STO with various Pr content ($x=0$, $1/3$, $1/2$, and 1) measured along the respective in-plane [001] and [1-10] directions. Figure 1(a) shows the ferromagnetic (FM)–antiferromagnetic (AF) transition at 160 K in NSMO films ($x=0$) along both directions. In addition, Fig. 1(e) proves the first-order MI transition with thermal hysteresis that has been unattainable previously in the tetragonally modified films. The transport properties are also slightly anisotropic in that the resistivity (ρ) along [001] direction is higher than that along the [1-10] direction consistent with the anisotropy in magnetic hysteresis loops (not shown). Upon increasing the Pr content x, the AF state gradually turned into a canted FM state preferentially along the [001] direction, as described in Fig. 1(c) ($x=1/2$) and Fig. 1(d) ($x=1$, PSMO). The anisotropic magnetic properties are manifested for $x \geqslant 1/2$, indicating that the magnetic easy axis is [001]. In contrast, magnetic properties in A-type $Nd_{0.45}Sr_{0.55}MnO_3$ twin-free bulk single crystals show substantially identical AF below T_N along any crystallographic axes.[14] Thus the emerging ferromagnetism along [001] in PNSMO ($x=1/2$) and PSMO ($x=1$) should be ascribed to the anisotropic strain in the epitaxial films, which implies the recovery of the spin-orbit coupling due to the e_g-orbital degeneracy once suppressed by JT distortion for low x values. Furthermore, $\rho_{[001]}$ becomes lower than $\rho_{[1\text{-}10]}$ with increasing Pr content x. In this manner, the anisotropic crossover between $1/3 < x < 1/2$ is demonstrated both in the magnetic and transport properties.

Figure 2 exhibits the transport data including a magnetic-field induced insulator-metal transition for the NPSMO films on STO [Figs. 2(a)–2(d)] and LSAT [Figs. 2(e)–2(h)] substrates measured along the [001] direction. Films on LSAT have in-plane isotropic magnetic and transport properties. In the case of $x=0$ [Figs. 2(a) and 2(e)], NSMO films on STO substrates show a large change in resistivity by an application of a magnetic field similar to those of bulk single crystals due to the collapse of the CO. Meanwhile, NSMO films on LSAT are modified into a rather metallic state with a trace of hysteresis, which is quite similar to that of the $(Nd_{0.5}La_{0.5})_{0.5}Sr_{0.5}MnO_3$ bulk single crystals.[24] The change in the strain effect in switching from STO to LSAT substrate

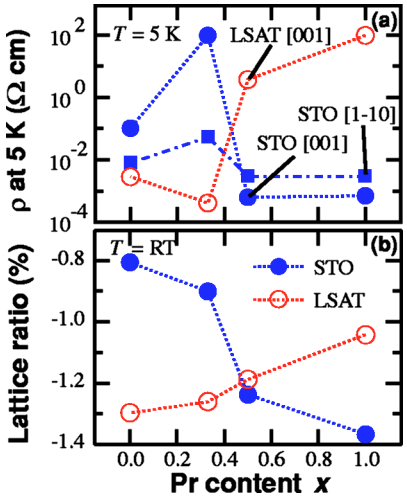

FIG. 3. (Color online) (a) ρ at 5 K of NPSMO films on STO and LSAT substrates are plotted. (b) Lattice ratios of $[\sqrt{2}d(1\text{-}10) - d(001)]/d(001)$ for STO (110) and $[\sqrt{2}d(110) - d(001)]/d(001)$ for LSAT (110) at RT.

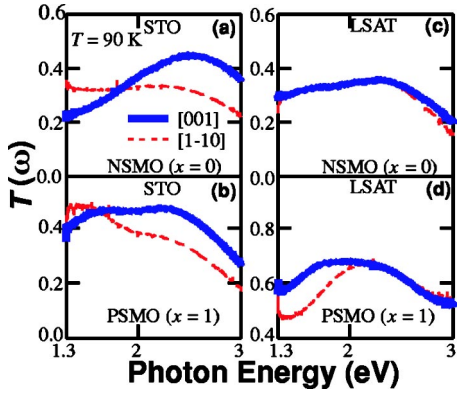

FIG. 4. (Color online) The optical transmittance spectra $[T(\omega)]$ at 90 K in the range of 1.3 eV$<\hbar\omega<$3.0 eV for the NSMO (a) and PSMO (b) films on STO were displayed in left panels. $[T(\omega)]$ is divided by that of the respective bare substrates. $[T(\omega)]$ for the NSMO (c) and PSMO (d) films on LSAT were shown in right panels.

is thus equivalent to the increasing of the one-electron bandwidth for NSMO films. As Pr content x increases to 1/3 [Figs. 2(b) and 2(f)], the trend of the CO insulating state on STO and the metallic state on LSAT becomes obvious. The trend, however, is completely reversed upon reaching $x=1/2$ [Figs. 2(c) and 2(g)]; a metallic state emerges for the films on STO and insulating behavior with large thermal hysteresis and large magnetoresistance on LSAT. At the PSMO ($x=1$) end [Figs. 2(d) and 2(h)], films on STO and LSAT show the largest disparity. While the films on STO show the metallic canting state as described in Fig. 1, a sharp MI transition is observed for the films on LSAT. This is a strain-induced crossover of the MI transition, because this crossover cannot be understood without the strain effect on the change in one-electron bandwidth other than the simple difference of the ionic radii between Nd and Pr ions. In addition, a magnetic field of 3 T is sufficient to cause an abrupt transition with the field-cooling process, in contrast to the 6 T necessary for the bulk crystal transition.[20] The large reduction of the threshold magnetic field into the metallic state is attributed to the strain effect. This is to be distinguished from random field effects frequently reported in polycrystalline thin films arising from the disorder.[25]

To gain some insight into the mechanism of the crossover, we summarize the resistivity (ρ) at 5 K (representing the ground state) and specific lattice constant ratios measured at RT with respect to the Pr content x in Fig. 3. An approximate correlation is seen between the x dependence of ρ and that of the specific lattice ratios such as $[\sqrt{2}d(1\text{-}10) - d(001)]/d(001)$ for the films on STO and $[\sqrt{2}d(110) - d(001)]/d(001)$ for the films on LSAT in Fig. 3(b). The ratio $[\sqrt{2}d(1\text{-}10) - d(001)]/d(001)$ is the in-plane anisotropy for films on STO due to the anisotropic lattice relaxation. The other lattice ratio describes the out-of-plane lattice deformation relative to the in-plane lattice constant, which is also a variable for films on (001) substrates. However, the variety of mode of deformation for the (110)-oriented epitaxial films is distinguished from that for the films being forced by the in-plane tetragonal symmetry of the (001) substrate. That is, one can have different values of $d(100)$ and $d(010)$ for a given $d(110)$ because the bond angle between [100] and [010] is also a variable. Since the OO plane such as (100) or (001) does not lie on the (110) substrates, the easily deformable anisotropic JT distortion [e.g., $d(100) \neq d(001)$] that is necessary for the OO is crucial in achieving the MI transition. It is quite clear that the flexibility in the mode of deformation for the films grown on a (110) substrate is the key for realizing the sharp first-order phase transitions. Despite the lack of detailed theoretical studies that take the nontetragonal distortions into account explicitly, we can thus argue together with the assignment of the OO planes below that the strain physics is well presented in the correlation in Fig. 3.

The evidence that the OO lies out of the sample plane is provided by the optical transmission spectroscopy. Figure 4 presents the anisotropic optical transmittance spectra $[T(\omega)]$ at 90 K ($<T_{co}$) in the range of 1.3 eV$<\hbar\omega<$3.0 eV for the films on STO and LSAT substrates, respectively. In the previous optical studies using twin-free single crystals,[13] the anisotropic optical conductivity, which translates into the absorbance in our measurement, constantly shows a reversal of the anisotropy in the visible region; the direction of the stronger absorption in the IR side of the crossing corresponds to the orientation of the orbital. The transmittance spectra in Fig. 4 also show very similar feature to the bulk single crystals. We therefore work on the premise that the direction with the lower transmittance in the low-energy side of the anisotropy crossing corresponds to the direction of the orbital. Figures 4(a) and 4(b) show that at least one lobe of orbitals is along [001] and not along [1-10]. In the (*Pbnm*) setting, [001] is the c axis in which orbitals do not lie. However, $d(001)$ is rather elongated due to the substrate strain and $d(100)$ is much shorter than $d(001)$.[26] We should thus assign [100] to be the c axis and conclude that the OO lies in (100) plane for the films on STO. This agrees with the overall anisotropy of the films on STO in the higher Pr content. In particular, that magnetic easy axis is [001] for PSMO films

on STO can be naturally understood on the condition that OO lies in (100) plane, by taking into account of the layered metallic nature of *A*-type AFM. The rather isotropic and insulating ground state in NSMO on STO suggests the *CE*-type order. The in-plane anisotropy in films on STO thus reflects the *A*-type/*CE*-type crossover. In the case of the films on LSAT, (001) is a possible OO plane in the PSMO side [Fig. 4(d)]. However, we cannot compare the in-plane lattice constant because the length of $d(001)$ is fixed to that of $\sqrt{2}d(1\text{-}10)$ due to the coherent growth. Therefore further optical measurements into the far IR region are necessary to confirm that the OO plane is (100) or (001) in this case.

In conclusion, we have demonstrated the strain physics in perovskite manganite epitaxial thin films evidenced as the anisotropic and substrate-dependent crossover of the MI transition utilizing the "tetragonal symmetry breaking." The substrate-induced strain is a powerful tool for the control of the MI transition by tuning the one-electron bandwidth through the JT distortion. By a proper choice of the substrate symmetry and lattice parameters, the phase competition can be sensitively modulated, bringing out a gigantic response. We believe that the results in this paper are valuable in paving the way to the strongly correlated electron devices that utilize the oxide superlattices and interfaces comprised of the COO materials as well as understanding the strain physics in manganites.

Y.O. thanks Y. Tomioka for showing unpublished data and for enlightening comment, and M. Kawasaki and Y. Tokura for inspiring advice. We acknowledge S. Koh for the use of the x-ray diffractometer. The financial support to M.N. and N.T. by the 21st Century COE Program for "Applied Physics on Strong Correlation" is also appreciated. This work was supported by JSPS, KAKENHI(15104006).

*Electronic address: y_ogimoto@mac.com

[1] Y. Tomioka, A. Asamitsu, Y. Moritomo, and Y. Tokura, J. Phys. Soc. Jpn. **64**, 3626 (1995).
[2] Y. Tokura, *Colossal Magnetoresistive Oxides* (Gordon and Breach Science Publishers, London, 2000).
[3] Y. Tokura and N. Nagaosa, Science **288**, 462 (2000).
[4] M. J. Calderon, A. J. Millis, and K. H. Ahn, Phys. Rev. B **68**, 100401(R) (2003).
[5] K. H. Ahn, T. Lookman, and A. R. Bishop, Nature (London) **428**, 401 (2004).
[6] Y. Suzuki, H. Y. Hwang, S.-W. Cheong, and R. B. van Dover, Appl. Phys. Lett. **71**, 140 (1997).
[7] J. N. Eckstein, I. Bozovic, J. O'Donnell, M. Onellion, and M. S. Rzchowski, Appl. Phys. Lett. **69**, 1312 (1996).
[8] Y. Konishi, Z. Fang, M. Izumi, T. Manako, M. Kasai, H. Kuwahara, M. Kawasaki, K. Terakura, and Y. Tokura, J. Phys. Soc. Jpn. **68**, 3790 (1999).
[9] Y. Tomioka and Y. Tokura, Phys. Rev. B **66**, 104416 (2002).
[10] S. Murakami and N. Nagaosa, Phys. Rev. Lett. **90**, 197201 (2003).
[11] Z. Fang, I. V. Solovyev, and K. Terakura, Phys. Rev. Lett. **84**, 3169 (2000).
[12] Y. Ogimoto, M. Izumi, T. Manako, T. Kimura, Y. Tomioka, M. Kawasaki, and Y. Tokura, Appl. Phys. Lett. **78**, 3505 (2001).
[13] K. Tobe, T. Kimura, and Y. Tokura, Phys. Rev. B **69**, 014407 (2004).
[14] H. Kuwahara, T. Okuda, Y. Tomioka, A. Asamitsu, and Y. Tokura, Phys. Rev. Lett. **82**, 4316 (1999).
[15] H. Kuwahara, Ph.D. thesis, University of Tokyo, 1997.
[16] M. Kasai, H. Kuwahara, Y. Moritomo, Y. Tomioka, and Y. Tokura, Jpn. J. Appl. Phys. **35**, L489 (1996).
[17] H. Kuwahara, Y. Tomioka, A. Asamitsu, Y. Moritomo, and Y. Tokura, Science **270**, 961 (1995).
[18] H. Kawano, R. Kajimoto, H. Yoshizawa, Y. Tomioka, H. Kuwahara, and Y. Tokura, Phys. Rev. Lett. **78**, 4253 (1997).
[19] R. Kajimoto, H. Yoshizawa, H. Kawano, H. Kuwahara, Y. Tokura, K. Ohoyama, and M. Ohashi, Phys. Rev. B **60**, 9506 (1999).
[20] Y. Tomioka, A. Asamitsu, Y. Moritomo, H. Kuwahara, and Y. Tokura, Phys. Rev. Lett. **74**, 5108 (1995).
[21] R. Kajimoto, H. Yoshizawa, Y. Tomioka, and Y. Tokura, Phys. Rev. B **66**, 180402(R) (2002).
[22] M. Kawasaki, K. Takahashi, T. Maeda, R. Tsuchiya, M. Shinohara, O. Ishiyama, T. Yonezawa, M. Yoshimoto, and H. Koinuma, Science **266**, 1540 (1994).
[23] Note that the mixture of two types of domains maintains overall twofold in-plane anisotropy. Therefore, anisotropic physical properties governed by a symmetric second rank tensor are preserved in the mixture.
[24] Y. Moritomo, H. Kuwahara, Y. Tomioka, and Y. Tokura, Phys. Rev. B **55**, 7549 (1997).
[25] Z. Q. Yang, R. W. A. Hendrikx, P. J. M. v. Bentum, and J. Aarts, Europhys. Lett. **58**, 864 (2002).
[26] $[d(001)-d(100)]/d(100)$ for the films on STO was in the range of 0.32–0.45 %.